Wavelength Dependence for the Photoreactions of DNA–Psoralen Monoadducts. 1. Photoreversal of Monoadducts†

Yun-bo Shi and John E. Hearst*

Department of Chemistry, University of California, Berkeley, Berkeley, California 94720

Received September 23, 1986; Revised Manuscript Received February 3, 1987

ABSTRACT: We have studied the wavelength dependence for the photoreversal of a monoadducted psoralen derivative, HMT [4′-(hydroxymethyl)-4,5′,8-trimethylpsoralen], in a single-stranded deoxyoligonucleotide (5′-GAAGCTACGAGC-3′). The psoralen was covalently attached to the thymidine residue in the oligonucleotide as either a furan-side monoadduct, which is formed through the cycloaddition between the 4′,5′ double bond of the psoralen and the 5,6 double bond of the thymidine, or a pyrone-side monoadduct, which is formed through the cycloaddition between the 3,4 double bond of the psoralen and the 5,6 double bond of the thymidine. As a comparison, we have also investigated the wavelength-dependent photoreversal of the isolated thymidine–HMT monoadducts. All photoreversal action spectra correlate with the extinction spectra of the isolated monoadducts. In the case of the pyrone-side monoadduct, two absorption bands contribute to the photoreversal with a quantum yield of 2×10^{-2} at wavelengths below 250 nm and 7×10^{-3} at wavelengths from 287 to 314 nm. The incorporation of the monoadduct into the DNA oligomer had little effect upon the photoreversal rate. For the furan-side monoadduct at least three absorption bands contribute to the photoreversal. The quantum yield varied from 5×10^{-2} at wavelengths below 250 nm to 7×10^{-4} at wavelengths between 295 and 365 nm. In contrast to the case of the pyrone-side monoadduct, the incorporation of the furan-side monoadduct into the DNA oligomer reduced the photoreversal rate constant at wavelengths above 285 nm.

The ability of psoralens to cross-link two strands of double-stranded nucleic acid has resulted in their widespread use in the treatment of human skin diseases (Fitzpatrick et al., 1982; Parrish et al., 1982) and in their use as probes of nucleic acid secondary and tertiary structures [for reviews, see Song and Tapley (1979) and Cimino et al., (1985)]. They have also been used in probing the interactions between different nucleic acids, such as between the U4 and U6 RNAs in U4/U6 ribonucleoprotein complexes (Rinke et al., 1985) and between pre-mRNA and U1 or U2 RNP complex (Calvet et al., 1982; Setyono & Pederson, 1984), which are involved in pre-mRNA splicing (Krainer & Maniatis, 1985; Black et al., 1985). The mutagenic and lethal effects due to psoralen plus near-UV light (320–400 nm) have been studied in both prokaryotic and eukaryotic cells (Fujita, 1984; Cassier et al., 1984), and the nucleic acid lesions formed can be recognized by repair systems (Saffran & Cantor, 1984; Cassier et al., 1985; Bohr & Nielsen, 1984; Zhen et al., 1986; Van Houten et al., 1986a,b).

The chemical and photochemical properties of psoralens are well understood (Song & Tapley, 1979; Cimino et al., 1985; Parsons, 1980). They intercalate between base pairs of double-stranded nucleic acids (Isaacs et al., 1977, 1982). Upon UV irradiation (320–400 nm), the intercalated psoralens photoreact with pyrimidine bases to form pyrimidine–psoralen monoadducts (Straub et al., 1981; Kanne et al., 1982). Both the 4′,5′ double bond of the furan ring and the 3,4 double bond of the pyrone ring of a psoralen can react with the 5,6 double bond of a pyrimidine base. If the 4′,5′ double bond reacts, a furan-side monoadduct, M_{Fu},[1] is formed. On the other hand, if the 3,4 double bond reacts, a pyrone-side monoadduct, M_{Py}, is formed. Psoralens react primarily with thymidine in DNA and uridine in RNA and to a lesser extent with cytosine in both DNA and RNA (Turner & Noller, 1983; Garrett-Wheeler et al., 1984). The furan-side monoadduct, which absorbs photons of 320 nm or above, can be converted to a pyrimidine–psoralen–pyrimidine diadduct, which links the two nucleic acid strands together, with 320–400-nm light if there is an adjacent pyrimidine base on the other strand available for the photoreaction (Kanne et al., 1982; Gasparro et al., 1984). The pyrone-side monoadduct, however, cannot be driven to a diadduct with 320–400-nm light since it does not absorb light in this wavelength region. The exact structures of the adducts formed between thymidine and several psoralen derivatives are known from mass spectroscopy, proton NMR, and X-ray crystallography (Straub et al., 1982; Kanne et al., 1982; Peckler et al., 1982).

The adducts formed between nucleic acids and psoralens can be photoreversed. We have previously reported the action spectra for the photoreversal of the T (thymidine)–HMT [4′-(hydroxymethyl)-4,5′,8-trimethylpsoralen]–T diadduct and the same diadduct in an HMT-cross-linked double-stranded DNA oligomer (Cimino et al., 1986). We found that the photoreversal of the diadduct correlates with its absorption spectrum. The incorporation of the diadduct in a double-stranded DNA helix enhances the photoreversal below 290 nm where DNA bases absorb. Here we report the wavelength dependence for the photoreversal of T–HMT monoadducts (both M_{Fu} and M_{Py}) and the same monoadducts incorporated

† This work was supported by NIH Grant GM11180.

* Author to whom correspondence should be addressed.

[1] Abbreviations: HMT, 4′-(hydroxymethyl)-4,5′,8-trimethylpsoralen; EtOH, ethanol; ATP, adenosine 5′-triphosphate; EDTA, ethylenediaminetetraacetic acid; Tris, tris(hydroxymethyl)aminomethane; M_{Fu}, furan-side monoadduct; M_{Py}, pyrone-side monoadduct; 5′-[T-$(HMT)_{Fu}$]-3′, thymidine–HMT furan-side monoadduct with HMT on the 3′-side of the thymidine; 5′-[$T(HMT)_{Py}$]-3′, thymidine–HMT pyrone-side monoadduct with HMT on the 3′-side of the thymidine; T–HMT–T, thymidine–HMT–thymidine diadduct.

0006-2960/87/0426-3786$01.50/0

in a DNA oligonucleotide. We find again that the action spectra for the photoreversal of both M_{Fu} and M_{Py} are similar to the corresponding absorption spectra. The quantum yields for different absorption bands, however, are quite different. In the case of M_{Fu}, the incorporation of the monoadduct in DNA reduces the photoreversal rate constant at wavelengths above 285 nm. In the following paper (Shi & Hearst, 1987), we will report the wavelength dependence for the cross-linking of the DNA–HMT monoadducts in the presence of a complementary oligonucleotide.

Materials and Methods

Materials. HMT and [^{3}H]HMT (15.8 Ci/mmol) were gifts from HRI Associates Inc. (Berkeley, CA). Oligonucleotides were synthesized on an automated DNA synthesizer by the phosphotriester method (SAMONE DNA Synthesizer, Biosearch). After synthesis, the oligonucleotides were deprotected and purified by electrophoresis on a 20% polyacrylamide–7 M urea gel followed by EtOH precipitation. [γ-^{32}P]ATP and T4 polynucleotide kinase were obtained from Amersham. Poly[d(AT)] was purchased from Sigma.

Irradiations. The irradiation apparatus for both the broad-band (320–380 nm) and the monochromatic irradiations has been described in a previous paper (Cimino et al., 1986). The band width for all monochromatic irradiations was maintained constant at 2.5 nm. Monochromatic radiation was continuously monitored with an in-line photodiode, which was calibrated by actinometry with $K_3Fe(C_2O_4)_3$.

5′-End Labeling of DNA Oligonucleotides. Oligonucleotides with 5′-OH were labeled with [γ-^{32}P]ATP and T4 polynucleotide kinase and subsequently chased with cold ATP (Maniatis et al., 1982; Shi & Hearst, 1986). To label oligonucleotides with 5′-phosphate, the kinase exchange reaction was used (Maniatis et al., 1982). The kinase exchange solution (50 μL) containing ca. 3 μg of oligonucleotide, 0.15–0.3 mCi of [γ-^{32}P]ATP (3000 Ci/mmol), 5 μL of 10× exchange reaction buffer (0.5 M imidazole hydrochloride, 0.1 M $MgCl_2$, 50 mM dithiothreitol, 1 mM spermidine, 1 mM EDTA, pH 6.6), 3 μL of 5 mM ADP, and 11 units of T4 polynucleotide kinase was incubated at 37 °C for ca. 3 h. The reaction was stopped with an EtOH precipitation at −20 °C (10 mM $MgCl_2$, 0.2 M NaCl, 2.5 v/v EtOH). After the EtOH precipitation, the DNA was purified by 20% polyacrylamide–7 M urea gel electrophoresis. All the gels in this paper had a 30:1 acrylamide to *N,N′*-methylenebis(acrylamide) ratio and were run in 1× TBE buffer (50 mM Tris base, 50 mM boric acid, 1 mM EDTA, pH 8.3).

Preparation of Adducts. (*A*) *T–HMT Monoadducts.* T–[^{3}H]HMT–T diadduct was prepared from poly[d(AT)] and [^{3}H]HMT as described (Cimino et al., 1986). The diadduct (70 nmol in 2.6 mL of 9 mM KH_2PO_4–40 mM NaOAc buffer, pH 5) was photoreversed at 249 nm for 40 min (light intensity was 2.7×10^{14} photons/s). After photoreversal, the solution was concentrated in a Speedvac concentrator (Savant Instrument Inc.) to 1.5 mL and adjusted to pH 2. The photoreversal products were then isolated by loading the solution onto a 10 mm × 25 cm reverse-phase (C_{18}) HPLC column (Ultrasphere ODS, Altex-Beckman, Berkeley, CA) and eluting with a linear 10 mM KH_2PO_4 (pH 2.2)–CH_3OH gradient (Kanne et al., 1982; Cimino et al., 1986). The diadduct, furan-side monoadduct, pyrone-side monoadduct, and HMT eluted at 29, 39, 50, and 55 min, respectively. The purified adducts were then vacuum dried and redissolved back in an acetate buffer. About 3.5 nmol of M_{Fu} (in 50 mM NaOAc, 19 mM KH_2PO_4, pH 5.0) and 9.5 nmol of M_{Py} (in 40 mM NaOAc, 14 mM $KH_2PO.4$, pH 5.0) were thus obtained.

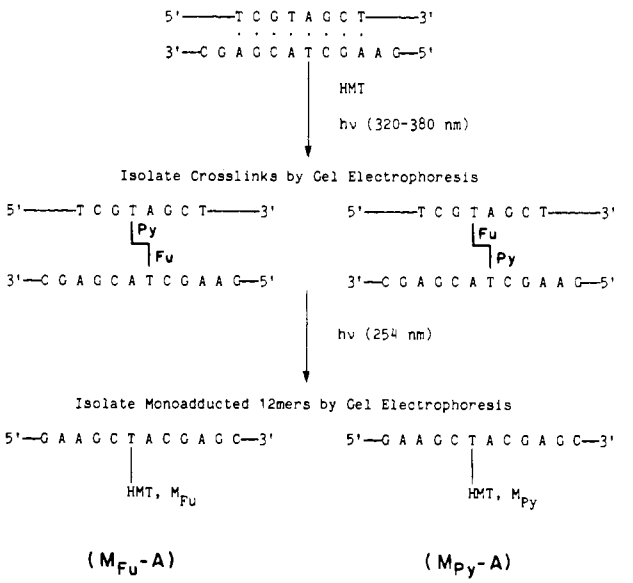

FIGURE 1: Preparation of DNA–HMT monoadducts. Abbreviations: M_{Fu}-A = 5′-GAAGC[T(HMT)$_{Fu}$]ACGAGC-3′; M_{Py}-A = 5′-GAAGC[T(HMT)$_{Py}$]ACGAGC-3′.

(*B*) *DNA–HMT Monoadducts.* The HMT-modified oligonucleotides used are 5′-GAAGCTACGAGC-3′ (oligonucleotide A) with an HMT molecule attached to the thymidine residue as either a furan-side monoadduct or a pyrone-side monoadduct, i.e., 5′-GAAGC[T(HMT)$_{Fu}$]-ACGAGC-3′ (M_{Fu}-A) or 5′-GAAGC[T(HMT)$_{Py}$]-ACGAGC-3′ (M_{Py}-A), respectively. They were prepared as described (Shi & Hearst, 1986). The procedures are outlined in Figure 1. Complementary oligonucleotides 5′-GAAGCT-ACGAGC-3′ (5′-^{32}P labeled at low specific activity) and 5′-TCGTAGCT-3′ were mixed with HMT under conditions where the double helix is stable and irradiated with 320–380-nm high-intensity broad-band light. Two cross-links were formed through the middle thymidine in each oligonucleotide, i.e., with either the furan end or the pyrone end attached to 5′-GAAGCTACGAGC-3′. The cross-links were isolated by electrophoresis on a 20% polyacrylamide-7 M urea gel. They were then photoreversed with 254-nm light from a low-pressure 40-W germicidal lamp, and the products were purified again by gel electrophoresis. The kinase exchange reaction described above was then used to label the DNA–HMT monoadducts, M_{Fu}-A and M_{Py}-A, before they were used.

Photoreversal of Adducts. (*A*) *T–HMT Monoadducts.* The photoreversals of the two monoadducts were conducted in a quartz cuvette of 1-cm path length at room temperature with monochromatic light. The solution was stirred, and the cuvette was covered with Parafilm during irradiation. The furan-side monoadduct (83 nM) was photoreversed in 20 mM NaOAc–0.4 mM KH_2PO_4, pH 5.0, and the pyrone-side monoadduct (88 nM) was photoreversed in 20 mM NaOAc–0.1 mM KH_2PO_4, pH 5.0. After photoreversal, the samples were run through a reverse-phase HPLC column with a linear 10 mM (pH 2.2) KH_2PO_4–CH_3OH gradient. The products were identified by their retention times on the column and quantified by ^{3}H scintillation counting.

(*B*) *DNA–HMT Monoadducts.* Both M_{Fu}-A and M_{Py}-A (2 nM) were photoreversed as above, but in 0.1 mM EDTA, pH 5.5. The photoreversed samples were dried in a Speedvac concentrator (Savant Instrument Inc.) without heating, dissolved in 5 M urea, 0.01% bromophenol blue, and 0.01% xylene cyanol FF loading buffer, and then electrophoresed on a 20% polyacrylamide–7 M urea gel (40 cm × 40 cm × 0.05 cm, 35 W for 3–4 h). Band positions of the monoadducted and un-

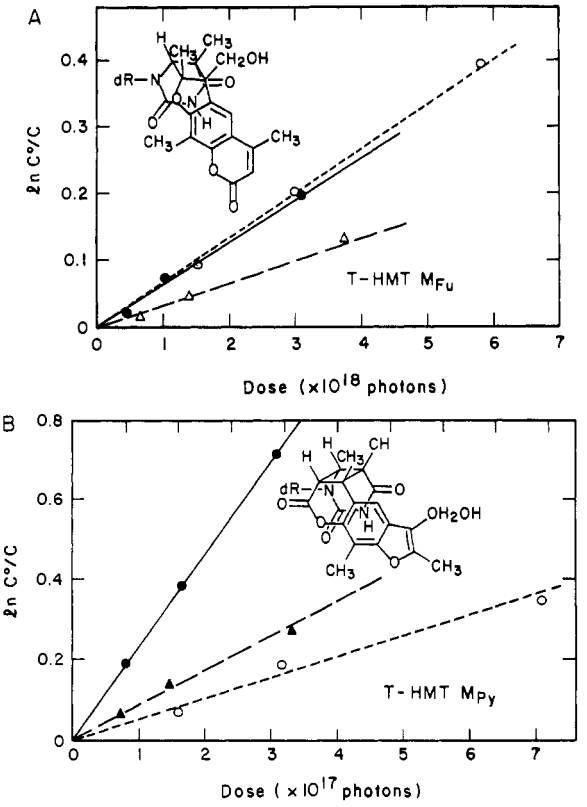

FIGURE 2: ln (C^0/C) vs. irradiation dose for the photoreversal of the T-HMT monoadducts. V = 750 μL; l = 1 cm. (A) Photoreversal of T-HMT furan-hside monoadducts (---) 334.3, (—) 287, and (--) 295 nm. The light intensities at 287, 295, and 334.3 nm are 3.80 × 10^{14}, 1.56 × 10^{15}, and 1.65 × 10^{15} photons/s, respectively. (B) Photoreversal of T-HMT pyrone-side monoadduct: (—) 240, (--) 265, and (---) 279 nm. The light intensities at 240, 265, and 279 nm are 3.42 × 10^{14}, 6.1 × 10^{13}, and 3.62 × 10^{14} photons/s, respectively.

modified oligonucleotides were located by autoradiography. The bands were then excised and quantified by Cerenkov counting with a Beckman LS-230 liquid scintillation counter.

The photoreversal of the adducts is first order with respect to the adduct concentrations. The photoreversal kinetics at low adduct concentrations can be analyzed as described by Cimino et al. (1986) to obtain the following relations:

$$C = C^0 \exp[-ktI_0l/(VN_0)] \quad (1)$$

$$k = 2.303\epsilon\phi \quad (2)$$

where k is the photoreversal rate constant [L/(einstein·cm)], I_0 is the light intensity (photons/s), V is the reaction volume (L), N_0 is Avogadro's number, l is the path length (cm), ϵ is the extinction coefficient of the adduct, ϕ is the quantum yield of photoreversal, and C^0 and C are the concentrations (mol/L, or M) of the adduct at time zero and at time t, respectively.

RESULTS

Photoreversal of the T-HMT Monoadducts. The monoadduct was photoreversed at pH 5.0, and the products were analyzed by HPLC. The photoreversal of T-HMT monoadducts yields thymidine and parent HMT, which can be photodamaged by UV irradiation. It is known that UV irradiation of aqueous solutions of HMT produces several damaged HMT compounds, including monomeric and dimeric products (Kao, 1984). Since we used T-[^{3}H]HMT, we could detect these damaged HMT compounds following the photoreversal of the monoadducts. In order to obtain the rate constant for the photoreversal of the monoadducts, the amounts of monoadducts remaining after photoreversal were determined by HPLC analysis, and the data were analyzed according to eq 1. Figure

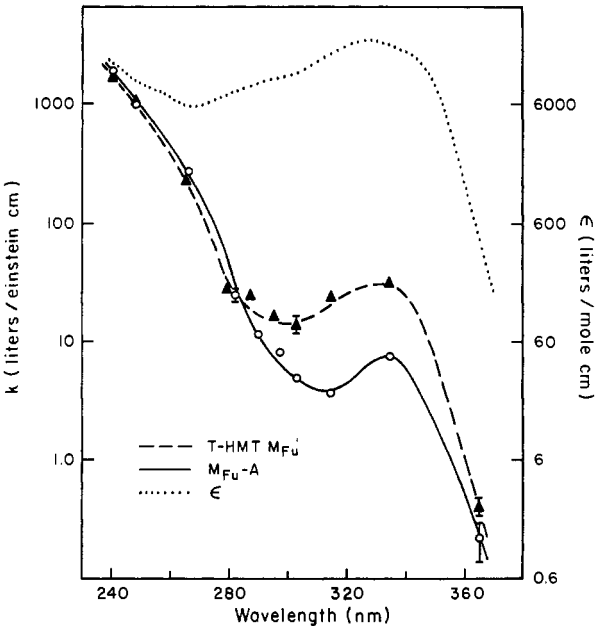

FIGURE 3: Action spectra for the photoreversal of the T-HMT and DNA-HMT furan-side monoadducts and the extinction spectrum of T-HMT furan-side monoadduct. The absorption of T-HMT M_{Fu} was measured with a Cary 118 spectrophotometer at room temperature in 50 mM NaOAc-19 mM KH_2PO_4, pH 5.0. M_{Fu}-A: see Figure 1. At 380 nm, the rate constants for both adducts are 0.

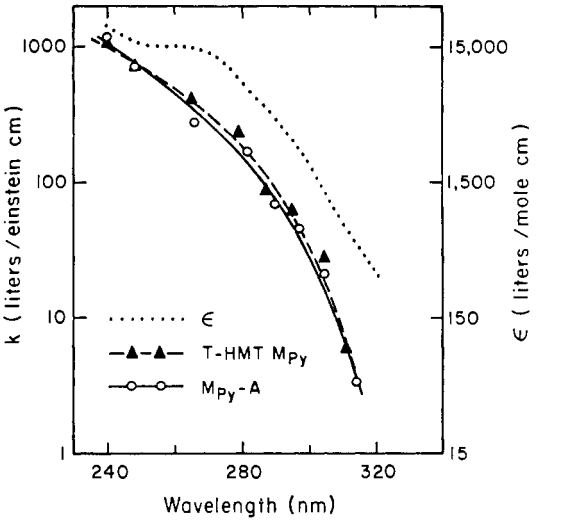

FIGURE 4: Action spectra for the photoreversal of the T-HMT and DNA-HMT pyrone-side monoadducts and the extinction spectrum of T-HMT pyrone-side monoadduct. The absorptions of T-HMT M_{Py} were measured with a Cary 118 spectrophotometer at room temperature in 50 mM NaOAc-14 mM KH_2PO_4, pH 5.0. M_{Py}-A: see Figure 1. At 334 nm, the rate constants for both adducts are 0.

2 shows the plots of ln (C^0/C) vs. irradiation dose for the two monoadducts at three different wavelengths. The rate constant k was calculated from the slope of the lines. The experiments were repeated at different wavelengths from 240 to 380 nm to obtain the action spectra for the photoreversals. The action spectrum for the furan-side monoadduct is shown in Figure 3. There is no detectable photoreversal at 380 nm. The action spectrum for the photoreversal of the pyrone-side monoadduct is shown in Figure 4; the photoreversal extends only to ca. 314 nm.

It is known that psoralen adducts with saturated 3,4 double bonds (in the pyrone-ring) can undergo pyrone-ring opening at high pH (Kanne et al., 1982; Cimino et al., 1986). It was also observed that under these conditions the photoreversal of the T-HMT-T diadduct and the same diadduct in a

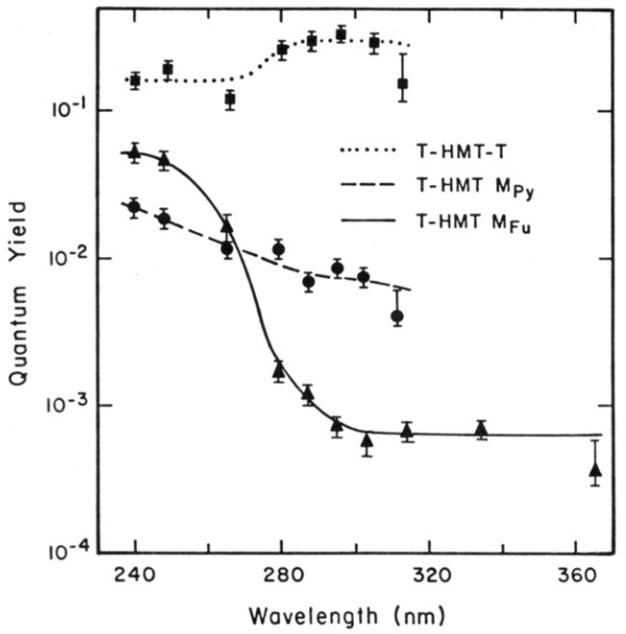

FIGURE 5: Quantum yields for the photoreversals of the T–HMT–T diadduct and the T–HMT monoadducts. The quantum yield for the photoreversal of the diadduct was estimated from the data of Cimino et al. (1986).

DNA–HMT cross-link is blocked at its pyrone end at wavelengths above 280 nm (Cimino et al., 1986). In order to ensure that only the pyrone-ring closed form of the pyrone-side monoadduct existed under the irradiation conditions, samples of the pyrone-side monoadduct in 10 mM KH_2PO_4, pH 2.2, were irradiated at 287 nm, and the products were analyzed as described above. The results were identical with those obtained at pH 5.0. Therefore, it is concluded that the action spectrum in Figure 4 is that for the pyrone-ring closed form of the monoadduct.

The quantum yield of photoreversal is related to the rate constant and the extinction coefficients of the monoadducts through eq 2. The extinction coefficients of the monoadducts were determined by measuring the absorption of the HPLC-purified T–[^{3}H]HMT monoadducts of known concentrations, which were determined by ^{3}H scintillation counting, and the resulting extinction spectra for the furan-side and pyrone-side monoadducts are shown in Figures 3 and 4, respectively. The quantum yield of the photoreversal of the monoadducts could then be calculated from the data in Figures 3 and 4, and the results are plotted in Figure 5. It can be seen that the action spectra of the photoreversal of the monoadducts correlate with their corresponding extinction spectra (Figures 3 and 4). The quantum yields, however, are different for different absorption bands. In the case of the pyrone-side monoadduct, two absorption bands contribute to the photoreversal with a quantum yield of 2×10^{-2} at wavelengths below 250 nm and 7×10^{-3} at wavelengths from 287 to 314 nm. For the furan-side monoadduct, at least three absorption bands contribute to the photoreversal. The quantum yield varies from 5×10^{-2} at wavelengths below 250 nm to 7×10^{-4} at wavelengths between 295 and 365 nm.

Photoreversal of DNA–HMT Monoadducts. The 5′-end labeled single-stranded DNA–HMT monoadducts, M_{Fu}-A and M_{py}-A, were photoreversed in 0.1 mM EDTA (pH 5.5) with monochromatic light. The products were analyzed by polyacrylamide gel electrophoresis. An autoradiogram of the time course of the photoreversal of M_{Fu}-A at 248 and 365 nm is shown in Figure 6. With increasing irradiation dose, the amount of M_{Fu}-A decreased, and the amount of the photo-

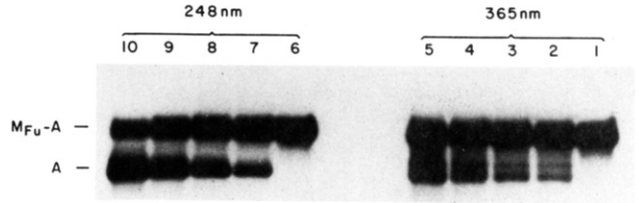

FIGURE 6: Photoreversal of M_{Fu}-A. $V = 750$ μL; $l = 1$ cm. M_{Fu}-A: see Figure 1. A = 5′-GAAGCTACGAGC-3′. (Lanes 1–5) Photoreversal at 365 nm, light intensity 1.1×10^{16} photons/s; lane 1, the dark control; lanes 2–5, samples exposed to 9.4×10^{19}, 1.42×10^{20}, 3.16×10^{20}, and 5.41×10^{20} photons, respectively. (Lanes 6–10) Photoreversal at 248 nm, light intensity 1.34×10^{15} photons/s: lane 6, the dark control; lanes 7–10, samples exposed to 8.0×10^{16}, 1.60×10^{17}, 3.20×10^{17}, and 6.40×10^{17} photons, respectively.

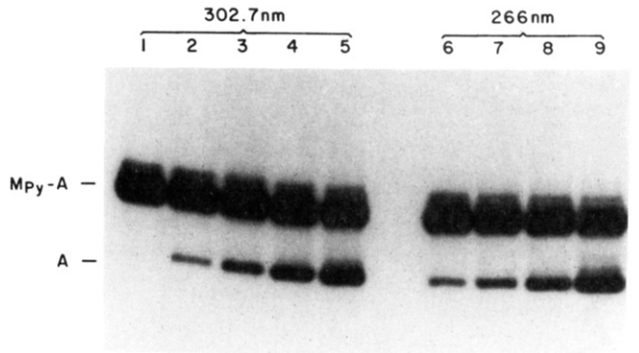

FIGURE 7: Photoreversal of M_{Py}-A. $V = 750$ μL; $l = 1$ cm. M_{Py}-A: see Figure 1. A: see Figure 7. (Lane 1) Dark control; (lanes 2–5), samples exposed to 9.0×10^{17}, 1.81×10^{18}, 3.60×10^{18}, and 7.0×10^{18} photons at 302.7 nm, respectively (light intensity was 7.5×10^{15} photons/s). (Lanes 6–9) Samples exposed to 7.2×10^{16}, 1.34×10^{17}, 2.57×10^{17}, and 6.9×10^{17} photons at 266 nm, respectively (light intensity was 1.72×10^{14} photons/s).

reversal product(s) increased. At wavelengths below 314 nm the photoreversal yielded only the unmodified oligonucleotide A. At wavelengths above 314 nm, however, another photoproduct was also produced, as seen in the figure for the irradiation at 365 nm. The product has not been characterized, but we assume that it is some sort of damaged DNA, since irradiating the product (purified from the gel) at 254 nm did not change its mobility on the gel (data not shown), suggesting it does not contain an HMT moiety. The damage must be due to the absortion of the HMT monoadduct or parent HMT generated during the irradiation because DNA bases do not absorb light above 314 nm. Since there are several absorption bands in the wavelength region (240–380 nm) for both the monoadducted HMT and the parent HMT, the photoreactions at different wavelengths could be quite different. Therefore, the unidentified photoproduct could be generated through either a one-photon process or a two-photon process. In the first case, the excited HMT moiety causes DNA damage upon leaving the DNA. In the second case, the monoadduct is photoreversed first, and the parent HMT thus generated acts as a DNA sensitizer, thereby causing damage. No attempt has been made to distinguish between these possibilities.

Figure 7 shows an autoradiogram of the time course of the photoreversal of M_{Py}-A at 266 and 302.7 nm. Again, with increasing dose the photoreversal product(s) increased and M_{Py}-A decreased (this is not easily visible in the figure due to overexposure of the film). The band moving slower than M_{Py}-A is a damaged product generated during the storage of M_{Py}-A and constituted a few percent of the total ^{32}P counts. Also seen in the figure are products other than the unmodified oligonucleotide A. The amounts of these products varied with wavelength; more damaged products were generated at shorter

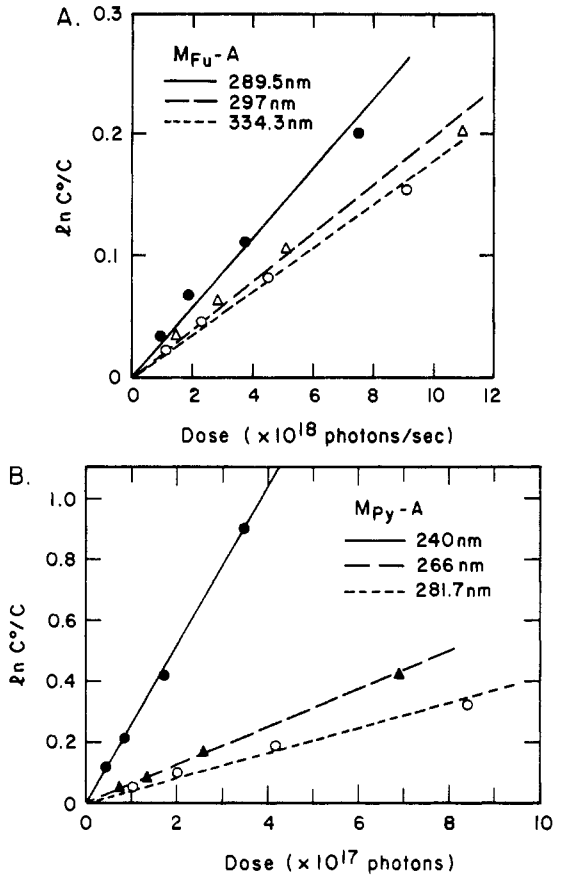

FIGURE 8: ln (C^0/C) vs. irradiation dose for the photoreversal of the DNA–HMT monoadducts. V = 750 μL; l = 1 cm. (A) Photoreversal of M_{Fu}-A. The light intensities at 289.5, 297, and 334.3 nm were 3.91×10^{15}, 5.76×10^{15}, and 1.88×10^{15} photons/s, respectively. (B) Photoreversal of M_{Py}-A. The light intensities at 240, 266, and 281.7 nm were 3.57×10^{14}, 1.72×10^{14}, and 1.72×10^{15}, respectively.

wavelength. We did not identify these products.

The photoreversal data were analyzed by determining the amount of DNA–HMT monoadducts remaining after photoreversal. This was done by excising the bands and quantifying them by ^{32}P Cerenkov counting. The data were then plotted according to eq 1. The plots of ln (C^0/C) vs. irradiation dose at three different wavelengths for M_{Fu}-A and M_{Py}-A are shown in Figure 8. The photoreversal rate constants were determined from plots such as these. The experiments were repeated at different wavelengths from 240 to 380 nm to obtain the action spectra for the photoreversals. Again no photoreversal was detected at 334 nm for M_{Py}-A and at 380 nm for M_{Fu}-A. The action spectra for M_{Fu}-A and M_{Py}-A are shown in Figures 3 and 4, respectively. Compared to the action spectra for the photoreversal of T–HMT monoadducts, it can be seen that the incorporation of the T–HMT pyrone-side monoadduct into the oligonucleotide has little effect upon the photoreversal rate constant. However, the incorporation of the T–HMT furan-side monoadduct into the oligonucleotide reduces the photoreversal rate constant at wavelengths above 285 nm. Below this wavelength the photoreversal rate constant is identical for the T–HMT and DNA–HMT furan-side monoadducts.

The reciprocity of the photoreversal of M_{Fu}-A was confirmed by exposing identical samples to a constant light dose (5.1×10^{18} photons) at 297 nm. The light intensity seen by each sample was varied by threefold. The irradiation times were varied correspondingly to maintain the constant dose. All irradiated samples photoreversed to an identical extent. Thus under our irradiation conditions, the photoreversal is dependent only on the total irradiation dose and independent of the light intensity. The reaction is, therefore, a one-photon process. Similar experiments were done for the photoreversal of M_{Py}-A. Again, it was found that the photoreversal was a one-photon process.

Discussion

Quantum Yield of the Photoreversal of the T–HMT Monoadducts. As shown in Figures 3 and 4, in the wavelength region from 240 to 380 nm there are at least three absorption bands for T–HMT furan-side monoadduct and two absorption bands for T–HMT pyrone-side monoadduct. The action spectra for the monoadducts in Figures 3 and 4 are clearly similar in shape to the extinction spectra of the corresponding monoadducts. The quantum yields are different for different absorption bands (Figure 5). For the pyrone-side monoadduct, the photoreversal in the shorter wavelength band is about 3 times more efficient than the photoreversal in the longer wavelength band. The quantum yield is 2×10^{-2} below 250 nm and 7×10^{-3} from 287 to 314 nm. In the case of the furan-side monoadduct, the quantum yields for different absorption bands differ by up to factor of 70. The quantum yield at wavelengths below 250 nm is 5×10^{-2}, whereas at wavelengths between 295 and 365 nm it is only 7×10^{-4}.

Also shown in Figure 5 is the quantum yield for the photoreversal of T–HMT–T diadduct, which was estimated from the data of Cimino et al. (1986). It is apparent that the photoreversal of the diadduct is much more efficient than those of the monoadducts at all wavelengths where the diadduct absorbs. This indicates that the electronic properties and/or steric constraints are quite different for the diadduct and the monoadducts. It is known that thymidine dimers can be photoreversed at wavelengths below 260 nm with a quantum yield of about unity (Deering & Setlow, 1963). Therefore, the absorption of the thymidine moieties in the monoadducts can also contribute to the photoreversal of the monoadducts. It has been proposed that the photoreversal of the diadduct below 260 nm is predominantly through the absorption of the thymidine moieties in the diadduct (Cimino et al., 1986). If this is also true for the photoreversal of the monoadducts, then it is easy to explain the greater quantum yields for the photoreversal of the monoadducts at wavelengths below 250 nm, since the photoreversal through the excitation of the thymidine moiety is very efficient.

Effects of DNA Helix and Adjacent DNA Bases on the Photoreversal. Comparison of the photoreversal action spectra of T–HMT and DNA–HMT pyrone-side monoadducts in Figure 4 indicates that the single-stranded DNA helix and the adjacent DNA bases have no effect upon the photoreversal of the monoadduct. This is in contrast to the photoreversal of the DNA–HMT cross-link (Cimino et al., 1986), where the photoreversal of T–HMT–T was dramatically enhanced upon the incorporation of the diadduct into a double-stranded DNA helix at wavelengths below 288 nm. It was proposed that this enhancement was due to energy transfer from excited DNA bases to the psoralen moiety in the cross-link. The fact that the photoreversals of the T–HMT and DNA–HMT pyrone-side monoadducts are identical at all wavelengths suggests that energy transfer from nearby excited DNA bases to the psoralen group is inefficient in the single-stranded DNA helix. As shown in the accompanying paper (Shi & Hearst 1987), the photoreversal of the same DNA–HMT pyrone-side monoadduct is enhanced upon addition of the complementary oligonucleotide into the irradiation solution to form double-stranded DNA helix. This suggests that the photoreversal can be enhanced by efficient energy transfer from excited DNA bases in double-stranded but not single-stranded DNA and that the

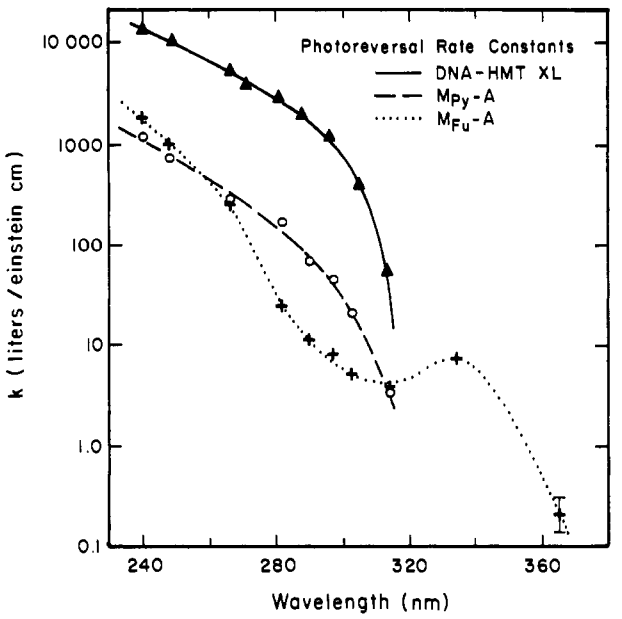

FIGURE 9: Action spectra for the photoreversal of DNA–HMT monoadducts and cross-link. The data for the cross-link are from Cimino et al. (1986).

pyrone-side monoadduct is stacked with DNA bases in the double helix.

In the case of furan-side monoadduct, again the DNA helix and the adjacent DNA bases have little effect on the photoreversal of the monoadduct at wavelengths below 285 nm, indicating that the energy transfer from DNA bases to the HMT group is inefficient. The photoreversal of the DNA–HMT monoadduct is, however, less efficient than that of the T–HMT furan-side monoadduct at wavelengths above 285 nm. The photoreversal of the furan-side monoadducts could occur via either the singlet excited state or the triplet excited state or both. The exact mechanism has not been established [for review, see Cimino et al. (1985)]. The triplet characteristics of several psoralen–nucleoside furan-side monoadducts and 4′,5′-dihydropsoralen derivatives have been determined (Blais et al., 1985; Land & Truscott, 1979). The quantum yield of triplet formation varies from 0.07 to 0.28 for the different adducts. These quantum yields are much larger than the quantum yield of the photoreversal of the furan-side monoadduct. Therefore, it is possible that the photoreversal occurs via the triplet state of the monoadduct. It is also known that thymine quenches the triplet states of psoralen–thymine furan-side monoadducts and 4′,5′-dihydropsoralen efficiently (Bensasson et al., 1980; Land & Truscott, 1979). Other nucleic acid bases can also quench the triplet states of 4′,5′-dihydropsoralen and coumarin, although less efficiently than thymine. Thus the decrease in the photoreversal rate constant above 285 nm upon the incorporation of the T–HMT furan-side monoadduct into oligonucleotide A could be due to the quenching of the triplet state of the monoadduct by adjacent DNA bases.

Comparison of Action Spectra for Photoreversal of DNA–HMT Monoadducts and Cross-Link. The action spectra for the photoreversals of M_{Fu}-A and M_{Py}-A are replotted in Figure 9 together with the action spectrum for the photoreversal of a DNA–HMT cross-link [data of Cimino et al. (1986)]. The photoreversal action spectra for H_{Fu}-A and M_{Py}-A are quite different due to the differences in both the absorption spectra of the adducts and the quantum yields of the photoreversals. While both M_{Py}-A and the cross-link are transparent to light above 320 nm, M_{Fu}-A can be photoreversed at wavelengths up to 365 nm. Below 320 nm, the photoreversal rate constant of the DNA–HMT cross-link is much larger than the photoreversal rate constants of the DNA–HMT monoadducts.

As we have described previously (Cimino et al., 1986; Shi & Hearst, 1986), site-specific placement of a psoralen molecule in a nucleic acid should facilitate elucidation of secondary and tertiary interactions in that nucleic acid. This is possible because the thermostability of the psoralen-monoadducted double-stranded nucleic acid is similar to that of the unmodified helix (Shi & Hearst, 1986), so the adduct should not perturb the native structure of the nucleic acid. Psoralen monoadduct, if in a double-stranded region, can be driven to a cross-link, which can be analyzed to yield information about the secondary and tertiary interactions in the nucleic acid (Thompson & Hearst, 1983). The results in this paper indicate that site-specific placement of a psoralen in a large DNA or RNA can be accomplished by psoralen transfer. As first suggested by Cimino et al. (1986), a monoadducted oligonucleotide containing a site-specific furan-side monoadduct or pyrone-side monoadduct can be prepared first. The monoadducted oligonucleotide can then be hybridized and cross-linked to its complement in a large nucleic acid. The cross-link can be photoreversed under conditions that favor the retention of the psoralen as a monoadduct on the large nucleic acid. Since the photoreversals of the monoadducts are much slower than that of the cross-link, the photoreversal can be controlled so that only the cross-link is photoreversed while very few monoadducts are photoreversed, allowing the accumulation of the monoadduct in the large nucleic acid. The resultant monoadduct can then function as a probe of local helical structure.

CONCLUSIONS

We report here the action spectra for the photoreversal of the two T–HMT monoadducts and the same monoadducts in a DNA oligonucleotide. We show that the incorporation of the pyrone-side monoadduct into the oligonucleotide had no effect upon the photoreversal. The incorporation of the furan-side monoadduct into the oligonucleotide, however, reduces the photoreversal rate constant at wavelengths above 285 nm, although the photoreversal rate constant remains unchanged at wavelengths below 285 nm. The quantum yields of the photoreversals of the two T–HMT monoadducts are quite different and vary considerably for photoreversal in different absorption bands.

ACKNOWLEDGMENTS

We thank Dr. G. D. Cimino, Dr. H. Gamper, and J. D. Kahn for helpful discussions and critical comments on the manuscript.

REFERENCES

Bensasson, R. V., Salet, C., Land, E. J., & Rushton, F. A. P. (1980) *Photochem. Photobiol. 31*, 129–133.

Black, D. L., Chabot, B., & Steitz, J. A. (1985) *Cell (Cambridge, Mass.) 42*, 737–750.

Blais, J., Ronfard-Haret, J. C., Vigny, P., Cadet, J., & Voituriez, L. (1985) *Photochem. Photobiol. 42*, 599–602.

Bohr, V., & Nielsen, P. E. (1984) *Biochim. Biophys. Acta 783*, 183–186.

Calvet, J. P., Meyer, L. M., & Pederson, T. (1982) *Science (Washington, D.C.) 217*, 456–458.

Cassier, C., Chanet, R., & Moustacchi, E. (1984) *Photochem. Photobiol. 39*, 799–803.

Cassier, C., Chanet, R., & Moustacchi, E. (1985) *Photochem. Photobiol. 41*, 289–294.

Cimino, G. D., Gamper, H. B., Isaacs, S. T., & Hearst, J. E. (1985) *Annu. Rev. Biochem. 54*, 1151–1193.
Cimino, G. D., Shi, Y.-B., Hearst, J. E. (1986) *Biochemistry 25*, 3013–3020.
Deering, R. A., & Setlow, R. B. (1963) *Biochim. Biophys. Acta 68*, 526–534.
Fitzpatrick, J. G., Stern, R. S., & Parrish, J. A. (1982) in *Psoriasis, Proceedings of the International Symposium, 3rd* (Farber, E. M., Ed.) pp 149–156, Grune and Stratton, New York.
Fujita, H. (1984) *Photochem. Photobiol. 39*, 835–839.
Garrett-Wheeler, E., Lockard, R. E., & Kumar, A. (1984) *Nucleic Acids Res. 12*, 3405–3423.
Gasparro, F. P., Saffran, W. A., Cantor, C. R., & Edelson, R L. (1984) *Photochem. Photobiol. 40*, 215–219.
Isaacs, S. T., Shen, C.-K. J., Hearst, J. E., & Rapoport, H. (1977) *Biochemistry 16*, 1058–1064.
Isaacs, S. T., Chun, C., Hyde, J. E., Rapoport, H., & Hearst, J. E. (1982) in *Trends in Photobiology* (Helene, C.,, Charlier, M., Monternay-Carestier, Th., & Laustriat, G., Eds.) pp 279–294, Plenum, New York.
Kanne, D., Straub, K., Hearst, J. E., & Rapoport, H. (1982) *J. Am. Chem. Soc. 104*, 6754–6764.
Kao, J. P.-Y. (1984) Ph.D. Thesis, University of California.
Krainer, A., & Maniatis, T. (1985) *Cell (Cambridge, Mass.) 42*, 725–736.
Land, E. J., & Truscott, T. G. (1979) *Photochem. Photobiol. 29*, 861–866.
Maniatis, T., Fritsch, E. F., & Sambrook, J. (1982) in *Molecular Cloning*, pp 125–127, Cold Spring Harbor Laboratory, Cold Spring Harbor, NY.
Parrish, J. A., Stern, F. S., Pathak, M. A. & Fitzpatrick, J. B. (1982) in *Science of Photomedicine* (Regan, J. D., & Parrish, J. A., Eds.) pp 595–623, Plenum, New York.
Parsons, B. J. (1980) *Photochem. Photobiol. 32*, 813–821.
Peckler, S., Graves, B., Kanne, D., Rapoport, H., Hearst, J. E., & Kim, S.-H. (1982) *J. Mol. Biol. 162*, 157–172.
Rinke, J., Appel, B., Digweed, M., & Luhrmann, R. (1985) *J. Mol. Biol. 185*, 721–731.
Saffran, W. A. & Cantor, C. R. (1984) *J. Mol. Biol. 178*, 595–609.
Setyono, B., & Pederson, T. (1984) *J. Mol. Biol. 174*, 285–295.
Shi, Y., & Hearst, J. E. (1986) *Biochemistry 25*, 5895–5902.
Shi, Y., & Hearst, J. E. (1987) *Biochemistry* (following paper in this issue).
Song, P. S., & Tapley, K. J., Jr. (1979) *Photochem. Photobiol. 29*, 1177–1197.
Straub, K., Kanne, D., Hearst, J. E., & Rapoport, H. (1982) *J. Am. Chem. Soc. 103*, 2347–2355.
Thompson, J. F., & Hearst, J. E. (1983) *Cell (Cambridge, Mass.) 32*, 1355–1365.
Turner, S., & Noller, H. F. (1983) *Biochemistry 22*, 4159–4164.
Van Houten, B., Gamper, H., Hearst, J. E., & Sancar, A. (1986a) *J. Biol. Chem. 261*, 14135–14141.
Van Houten, B., Gamper, H., Holbrook, S. R., Hearst, J. E., & Sancar, A. (1986b) *Proc. Natl. Acad. Sci. U.S.A. 83*, 8077–8081.
Zhen, W.-P., Jeppesen, C., & Nielsen, P. E. (1986) *Photochem. Photobiol. 44*, 47–51.

Wavelength Dependence for the Photoreactions of DNA–Psoralen Monoadducts. 2. Photo-Cross-Linking of Monoadducts†

Yun-bo Shi and John E. Hearst*
Department of Chemistry, University of California, Berkeley, Berkeley, California 94720
Received September 23, 1986; Revised Manuscript Received February 3, 1987

ABSTRACT: The photoreactions of HMT [4′-(hydroxymethyl)-4,5′,8-trimethylpsoralen] monoadducts in double-stranded DNA have been studied with complementary oligonucleotides. The HMT was first attached to the thymidine residue in the oligonucleotide 5′-GAAGCTACGAGC-3′ as either a furan-side monoadduct or a pyrone-side monoadduct. The HMT-monoadducted oligonucleotide was then hybridized to the complementary oligonucleotide 5′-GCTCGTAGCTTC-3′ and irradiated with monochromatic light. In the case of the pyrone-side monoadducted oligonucleotide, photoreversal was the predominant reaction, and very little cross-link was formed at all wavelengths. The course of the photoreaction of the double-stranded furan-side monoadducted oligonucleotide was dependent on the irradiation wavelength. At wavelengths below 313 nm, both photoreversal and photo-cross-linking occurred. At wavelengths above 313 nm, photoreversal of the monoadduct could not be detected, and photo-cross-linking occurred efficiently with a quantum yield of 2.4×10^{-2}.

The use of psoralens (furocoumarins) in the medical and bioloigical fields is highly dependent upon the ability of these compounds to cross-link double-stranded nucleic acids through photoreactions with adjacent pyrimidine bases on opposite strands. The cross-link formation is well understood and occurs in three steps (Song & Tapley, 1979; Parson, 1980; Parson, 1980; Cimino et al., 1985). First, psoralens intercalate between base pairs of a double-stranded nucleic acid. Second, the intercalated psoralens photoreact with pyrimidine bases to form psoralen–pyrimidine monoadducts under UV (320–400 nm) irradiation. Finally, the monoadducts photoreact with adjacent pyrimidine bases by absorbing a second photon to form diadducts that cross-link the two strands of the nucleic acid together. It has been well established that the furan-side monoadduct can be easily driven to a diadduct in a double-

† This work was supported by NIH Grant GM11180.
* Author to whom correspondence should be addressed.

0006-2960/87/0426-3792$01.50/0